

The NUSES space mission^(*)

P. SAVINA⁽¹⁾⁽²⁾ on behalf of the NUSES COLLABORATION

⁽¹⁾ *Gran Sasso Science Institute - Via Iacobucci 2, I-67100 L'Aquila, Italy*

⁽²⁾ *Istituto Nazionale di Fisica Nucleare (INFN), LNGS - I-67100 Assergi, L'Aquila, Italy*

received 2 December 2024

Summary. — The NUSES space mission aims to explore cosmic and gamma rays, high-energy astrophysical neutrinos, the Sun-Earth environment, space weather, and magnetosphere-ionosphere-lithosphere coupling (MILC). Additionally, NUSES aims to pave the way for future missions by testing new technologies and observational strategies. The satellite will carry two payloads: Terzina and Zirè. Zirè will measure the flux of electrons, protons, and light nuclei from a few to hundreds of MeV and evaluate new tools for detecting cosmic MeV photons and monitoring MILC signals. Terzina will monitor near-UV and visible light emissions from the Earth's limb to test the detection of Cherenkov light from extensive air showers produced by UHERCs or Earth-skimming high-energy neutrinos. This work will cover the current status of NUSES project design and its scientific and technological objectives.

1. – Introduction

The NUSES mission, led by Italy, is a pathfinder for novel observation methods and technologies to study high and low energy radiations from space, paving the way for new sensors and tools. Scheduled for launch in late 2025 under the management of the Italian Space Agency (ASI), the NUSES satellite will be a ballistic mission without orbital control, operating in a Low Earth Orbit (LEO) at an altitude of 535 km with a high inclination of 97.8° (LTAN = 18:00) in a Sun-synchronous orbit along the day-night boundary. NUSES hosts two payloads: Zirè [1] and Terzina [2]. Zirè will measure the flux ($E_{\text{kin}} < 300$ MeV) of cosmic electrons, protons, and light nuclei from solar and galactic sources; study cosmic radiation variability, including the Van Allen belt system; explore possible correlations with seismic activity via Magnetosphere-Ionosphere-Lithosphere Coupling (MILC); detect 0.1 - 30 MeV photons to study gamma sources. Terzina serves as a pathfinder for missions focused on ultra-high-energy (UHE) cosmic rays and neutrino astronomy using space-based atmospheric Cherenkov light detection. Each detector readout will use Silicon Photo Multipliers (SiPMs), replacing the conventional PhotoMultiplier Tubes (PMTs) used in space experiments. The innovative SiPM technology, used in both Zirè and Terzina, is chosen for its compact size and low power consumption. In this work, we present the two scientific payloads aboard the NUSES satellite.

^(*) IFAE 2024 - “Cosmology and Astroparticles” session

2. – The Zirè Experiment

The primary goal of the Zirè experiment is to detect Cosmic Rays with energies ranging from a few MeVs to hundreds of MeVs [3].

This aims to study their spectral features and to identify possible anomalies in the counting rates of trapped particles that could be linked to natural Earth events, such as earthquakes, volcanic eruptions, or strong Gamma Ray Bursts (GRBs).

Several ground-based and Low Earth Orbit (LEO) experiments have observed unexpected phenomena in the ionosphere, such as electromagnetic and plasma density perturbations, as well as an anomalous increase in low-energy electron and proton counting rates trapped in the Van Allen Belts (VABs) [4]. These observations can be theoretically explained by the Magnetospheric-Ionospheric-Lithospheric Coupling (MILC) model [5].

Studying low-energy Galactic Cosmic Rays also allows monitoring high-intensity solar particle emissions, as their energy spectrum is significantly influenced by solar activity, particularly for particles with rigidity below 10 GV. Solar activity follows an approximately 11-year cycle and includes transient phenomena such as solar flares and Coronal Mass Ejections (CMEs). These events emit Solar Energetic Particles (SEPs) with energies from a few tens of keV to a few GeV, which are accelerated and transported by the heliosphere, reaching Earth and causing space weather phenomena like geomagnetic storms.

The Zirè payload will also detect photons with energies from 0.1 MeV to a few tens of MeVs, enabling the study of transient events (Gamma Ray Bursts, electromagnetic follow-up of GW events, supernova emission lines, etc.) and steady gamma sources. With the instruments onboard Zirè, it is also possible to study correlations between bright GRBs and local effects on charged particles [6].

2.1. The Zirè Design. – A sectional view of the Zirè module design is shown in fig. 1. Starting from the left in fig. 1, the design comprises the following components:

- Three X-Y modules of the Fiber Tracker (FTK) with a $9.6 \times 9.6 \text{ cm}^2$ cross-section and 2.5 cm spacing. Each module consists of two planes, with the fibers in each plane orthogonal to those in the next [7].
- A tower of 32 Plastic Scintillator (PS) layers (PST), each composed of three PS X-Y bars. The first six PST layers, located below the FTK, measure $12 \times 12 \times 1 \text{ cm}^3$, while the remaining 26 layers are $12 \times 12 \times 0.5 \text{ cm}^3$.

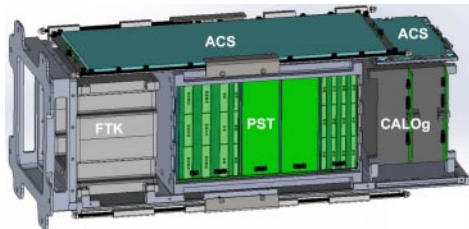


Fig. 1. – Preliminary mechanical design of the Zirè detector. Charged particles enter the detector from the left through a dedicated thin window, above FTK. Low-energy gamma-ray measurements are performed using two additional windows located near the CALOg (right and top side in the image, corresponding to the horizontal (H) and zenith (V) directions, respectively). The Low Energy Module (see text for more details) is not shown in this figure.

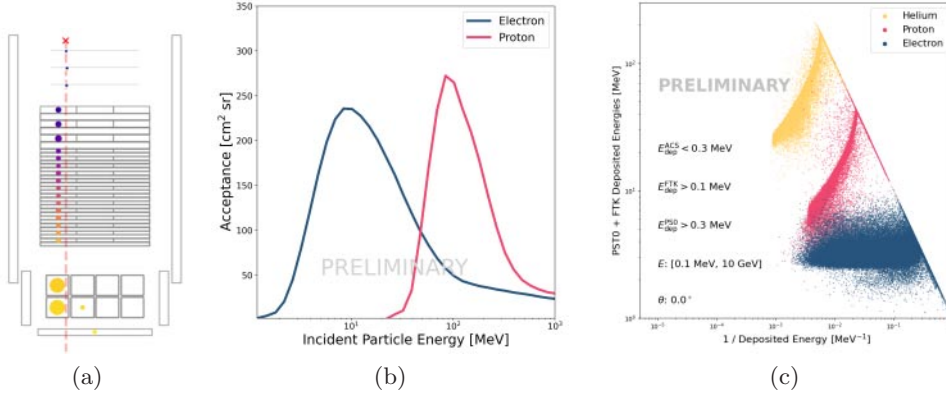


Fig. 2. – (a) Display of a simulated 1 GeV proton event crossing the Zirè detector, where the different detectors are shown in grey. The color from blue to yellow is proportional to the simulated trigger time of each sub-detector, while the marker size is proportional to the deposited energy. The dashed red line shows the track of the primary particle. (b) Preliminary effective acceptance for protons (red) and electrons (blue) obtained by selecting events satisfying a trigger and full containment requirement. (c) Total energy deposition inside the Fiber Tracker and the first layer of the PST (PS0) as a function of the inverse of the energy deposited inside the full instrument for contained electron (blue), proton (red), and helium (yellow) simulated events.

- A calorimeter (CALOG) made of a $4 \times 4 \times 2$ matrix of $2.5 \times 2.5 \times 3 \text{ cm}^3$ crystals. The two options considered for the crystals material are: Lutetium-yttrium orthosilicate (LYSO) crystals, or Gadolinium Aluminium Gallium Garnet (GAGG) crystals, both characterized by high light yield and fast response time.
- Nine PS layers, each 0.5 cm thick, forming an Anti-Coincidence System (ACS) that surrounds the instrument from all directions except the FTK side.

Monte Carlo (MC) simulations of incoming electron, proton, and helium events have been performed with a continuous energy spectrum from 100 keV up to 10 GeV. An example of a simulated proton event crossing the Zirè detector is shown in fig. 2(a). The produced MC dataset allowed an initial study of the detector’s performance, such as shower containment and effective acceptance. A preliminary estimate of the effective acceptance for both protons and electrons is shown in fig. 2(b), obtained by selecting events satisfying a trigger activation requirement consisting of an energy deposit greater than 0.1 MeV in the FTK and 0.3 MeV in the first PST layer (PS0), along with a full containment request. Additionally, from these simulated data, the particle identification capability for the Zirè module can be estimated from the energy deposit inside the FTK+PS0 as a function of the inverse of the total energy deposition inside the entire detector, as shown in fig. 2(c), where a separation between the different primary species is clearly observable.

The CALOG sub-detector will also be used independently for studying low-energy gamma rays in the range between 0.1 MeV and 50 MeV. Figure 3(a) shows a preliminary estimation of the effective area, summing the contributions of the two observing windows around the CALOG. The features in the curve and its general trend towards higher energies can be explained by the LYSO/GAGG absorption properties and the applied selection cuts.

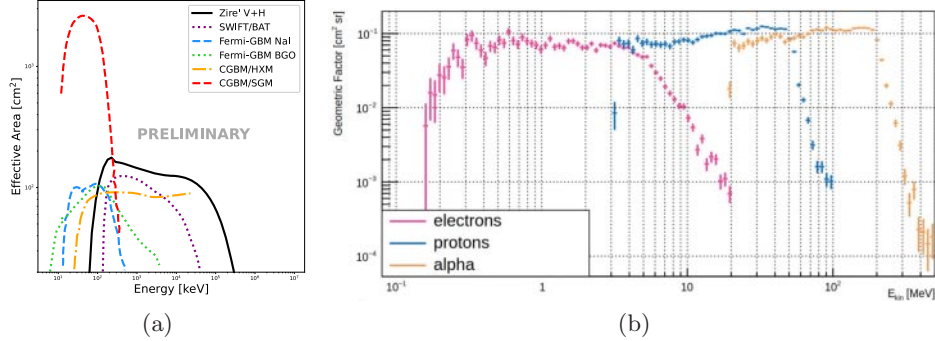


Fig. 3. – (a) Preliminary estimate of the Zirè (Vertical+Horizontal windows) effective area for gamma detection, along with the analogous curves from Fermi-GBM (NaI/BGO), CALET-GBM (HXM/SGM) and SWIFT/BAT [8]. (b) LEM Geometrical Factor. More details reported in the text.

A specific Zirè payload extension, named Low Energy Module (LEM) [9], will be designed for detecting low-energy electrons (with energies below 7 MeV) and protons (in the 3 MeV - 50 MeV range), which could provide greater sensitivity for MILC studies. The LEM module will be a particle spectrometer for time-resolved measurements of the differential flux distribution of low-energy charged particles. It will consist of five independent silicon detectors, a plastic calorimeter, two veto systems on top and at the bottom of the instrument, all surrounded by an aluminum mask with a scintillating collimator for the direction reconstruction of the incoming particle. An estimation of the geometrical factor of the LEM for electron (purple), proton (blue) and alpha (yellow) primaries is reported in fig. 3(b).

3. – The Terzina Experiment

Terzina is a telescope designed to detect Cherenkov light from extensive-air showers (EAS) induced by ultra-high-energy cosmic rays (UHECRs) and neutrinos in the Earth’s atmosphere. At energies above 1 PeV, tau and muon neutrinos passing through the Earth can produce μ and τ leptons, which may decay or interact in the atmosphere, resulting in Earth-skimming events. Cherenkov emission from an EAS is primarily due to high-energy ($E > 100$ MeV) electron-positron pairs generated during the shower. The number of Cherenkov photons is directly proportional to the shower energy, reflecting the energy of the primary particle initiating the cascade.

Terzina is expected to predominantly observe cosmic rays (CR) above the Earth’s limb [10], as their flux is significantly higher than that of neutrinos. The Cherenkov signals from these CR events share similar properties with those expected from neutrino events below the limb, including wavelength spectra, spatial profiles, and time distributions. Above-the-limb CR events are crucial for testing the components of an in-orbit Cherenkov telescope, such as optics, photo-sensors, electronics, and triggers. This strategy underpins the Terzina mission, aiming to validate the detection technique through in-orbit testing.

To estimate the expected signal in the Terzina telescope, we consider EAS generated by protons. Above-the-limb trajectories result in particle cascades at high altitudes in

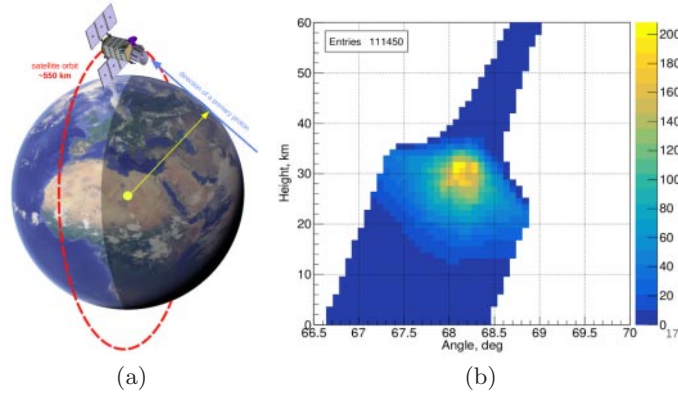


Fig. 4. – (a) Orbital configuration and geometry of an above-the-limb event. (b) Distribution of the detected Cherenkov photons from a 100 PeV proton EAS as a function of viewing angle and altitude above the limb.

a rarefied atmosphere. This limits the generation of optical Cherenkov emission but also reduces atmospheric attenuation during photon propagation. Detailed calculations of Cherenkov signal strength and geometry are necessary to determine the telescope’s sensitivity to these events. The results are presented in fig. 4. Cherenkov emission is observable from a thin atmospheric layer, with an angular size of less than 1° , corresponding to altitudes from 20 km to 50 km above the Earth’s limb (seen by Terzina at an elevation angle $\theta_d = 67.5^\circ$), as shown in fig. 4(b).

3.1. The Terzina Design. – The Terzina detector comprises a near-UV-optical telescope with Schmidt-Cassegrain optics and a Focal Plane Assembly (FPA), as shown in fig. 5.

The telescope’s optical system uses a dual mirror configuration with two parabolic mirrors: a primary mirror with a 394 mm radius and a secondary mirror with a 144 mm

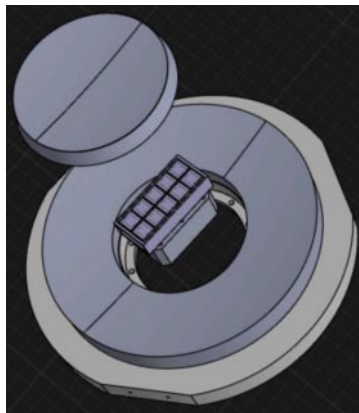


Fig. 5. – Optics scheme (M1, M2 primary and secondary mirrors) and FPA of Terzina with baffles to protect from stray light pollution.

radius, placed 280 mm apart. The FPA, with a maximum radius of 121 mm, is positioned 40 mm from the primary mirror. This setup maximizes the focal length to 925 mm in a compact telescope that fits within a $600 \times 600 \times 730 \text{ mm}^3$ envelope. The telescope operates inclined at 67.5° to the nadir, with the optical axis pointing towards the dark side of the Earth’s limb, achieving an expected duty cycle of around 40%. The star tracker system of the satellite platform maintains the optical axis configuration with high accuracy (0.1°). The total weight of the Terzina instrument (telescope and FPA) is about 35 kg.

The FPA, designed to detect photons from both below and above the limb, has a 2:5 aspect ratio and comprises 10 Silicon Photon Multipliers (SiPM) arrays of 8×8 pixels of size $r_{\text{SiPM}} \simeq 3 \text{ mm}$, forming 2 rows of 5 arrays each. The upper row (red area) observes events from below the Earth’s limb, performing background characterization, while the lower row (blue area) observes EAS events from above the limb. Terzina observes a large volume of the atmosphere, with a cross-section of $360 \times 140 \text{ km}^2$ across the Earth’s limb.

Given the focal length ($F_l = 925 \text{ mm}$) and the SiPM pixel size, the Field-of-View (FoV) per pixel is $\text{FoV}_{\text{pix}} = \arctan(r_{\text{SiPM}}/F_l) \simeq 0.18^\circ$, with a telescope FoV of 7.20° (40 pixels) along the Earth’s limb and 2.88° (16 pixels) across it.

The expected background radiation at Terzina’s operating altitudes, mainly due to electrons and protons in the 100 keV - 100 MeV range, can mimic events by producing Cherenkov emission within the telescope’s optical/mechanical parts.

The expected detector aperture for CR protons is reported in fig. 6, based on the BoL sensors’ response and a single threshold trigger scheme with $S_0 = 7 \text{ p.e.}$ Given the observed CR flux at energies exceeding 100 PeV, $\phi_{\text{CR}} \simeq 6.6 \times 10^3 \text{ km}^{-2} \text{ sr}^{-1} \text{ y}^{-1}$ [11], assuming a proton fraction of 50% [11], and a detector duty cycle of 40%, the derived aperture shows Terzina’s capability to observe a significant number of CR proton events (with $E \geq 100 \text{ PeV}$) within the first year of operation, estimating no less than 20 events per year.

4. – Conclusions

In this work, we have presented the NUSES mission and the two payloads mounted on the satellite: Zirè and Terzina. The Zirè detector onboard the NUSES satellite will contribute to the investigation of low energy Galactic Cosmic Rays and gamma rays

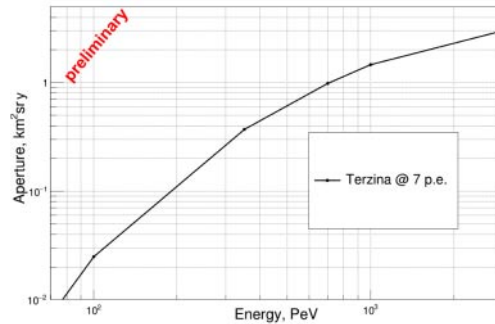


Fig. 6. – Expected terzina aperture as a function of the energy for proton-initiated shower during the first year of operation.

in the keV-MeV regime. Moreover, we have provided a preliminary estimation of the detection capabilities of the Terzina instrument. Both experiments will play a crucial role in the development and testing of advanced technologies, such as the SiPM-based one, for space detectors.

* * *

NUSES is funded by the Italian Government (CIPE n. 20/2019), by the Italian Minister of Economic Development (MISE reg. CC n. 769/2020), by the Italian Space Agency (CDA ASI n. 15/2022), by the Swiss National Foundation (SNF grant n. 178918) and by the European Union - NextGenerationEU under the MUR National Innovation Ecosystem grant ECS00000041 - VITALITY - CUP D13C21000430001.

REFERENCES

- [1] ALONSO F. M. *et al.*, *PoS*, **ICRC2023** (2023) 139.
- [2] ALOISIO R. *et al.*, *PoS*, **ICRC2023** (2023) 391.
- [3] DE MITRI I. *et al.*, *J. Phys.: Conf. Ser.*, **2429** (2023) 012007.
- [4] NEUBÜSER C. *et al.*, *Remote Sens.*, **15** (2023) 411.
- [5] PIESANTI M. *et al.*, *Remote Sens.*, **12** (2020) 3299.
- [6] BATTISTON R. *et al.*, *Astrophys. J. Lett.*, **946** (2023) L29.
- [7] NUSES COLLABORATION (MAZZIOTTA N. *et al.*), *PoS*, **ICRC2023** (2023) 083.
- [8] MEEGAN C. *et al.*, *Astrophys. J.*, **702** (2009) 791; YAMAOKA K. *et al.*, *PoS*, **ICRC2017** (2017) 614; BARTHELMI S. D. *et al.*, *Space Sci. Rev.*, **120** (2005) 143.
- [9] ALOISIO R. *et al.*, *PoS*, **ICRC2023** (2023) 1316.
- [10] BURMISTROV L. *et al.*, *EPJ Web of Conferences*, **283** (2023) 06006.
- [11] PIERRE AUGER COLLABORATION (ABREU P. *et al.*), *Eur. Phys. J. C*, **81** (2021) 966.